

Excited Leptons at the CERN Large Hadron Collider

O. J. P. Éboli¹, S. M. Lietti¹ and Prakash Mathews²

¹*Instituto de Física da USP,
C.P. 66.318, São Paulo, SP 05389-970, Brazil.*

²*School of Physics, University of Hyderabad,
Hyderabad 500 046, India.*

Abstract

We analyze the potential of the CERN Large Hadron Collider (LHC) to search for excited spin- $\frac{1}{2}$ electrons and neutrinos. Assuming an $SU(2)_L \otimes U(1)_Y$ invariant model, we study in detail the single production of excited electrons and neutrinos and respective backgrounds through the reactions $pp \rightarrow e^+e^-V$ and $e^\pm\nu V$ with $V = \gamma, W, \text{ or } Z$. We show that the LHC will be able to tighten considerably the direct constraints on these possible new states, probing excited lepton masses up to 1–2 TeV depending on their couplings to fermions and gauge bosons.

I. INTRODUCTION

The standard model (SM) of electroweak interactions explains very well the available experimental data [1]. Notwithstanding, some important questions are still left unanswered, in particular, the proliferation of fermionic generations and their complex pattern of masses and mixing angles are not explained by the model. A rather natural explanation for the replication of the fermionic generations is that the known leptons and quarks are composite [2] and they should be regarded as the ground state of a rich spectrum of fermions. Therefore, the observation of excited quarks and leptons would be an undeniable signal for compositeness [3].

Up to now all direct searches for compositeness have failed. At the DESY ep collider HERA [4], operating in the e^+p mode, no evidence of excited fermions was found which leads to 95% C.L. bounds $\mathcal{O}(200)$ GeV on the excited lepton mass for $m^* = \Lambda$, where we denote by Λ the strong dynamics scale. The direct search for single and pair productions of excited leptons at the CERN e^+e^- collider LEP leads to 95% C.L. constraints on m^* of the order $\mathcal{O}(100)$ GeV for $m^* = \Lambda$ [5].

In this work, we reexamine the single production of excited spin- $\frac{1}{2}$ electrons (e^*) and neutrinos (ν^*) at the LHC via the reactions

$$pp \rightarrow e^\pm e^{\star\mp} \rightarrow e^+ e^- V \quad , \quad (1)$$

$$pp \rightarrow \nu e^{\star\pm} + \nu^* e^\pm \rightarrow e^\pm \nu V \quad , \quad (2)$$

where V stands for γ , W^\pm or Z . We carefully analyze the SM backgrounds and signals for an $SU(2)_L \otimes U(1)_Y$ invariant model, which is described below. We show that the strongest limits are obtained for $V = \gamma$ and that the CERN Large Hadron Collider (LHC) will be able to probe for excited electrons and neutrinos with masses up to 1 TeV, assuming that $m^* = \Lambda$.

The outline of this paper is the following. In section II we review the model used in our analysis. Section III contains our results while the conclusions are presented in Section IV.

II. MODEL

The strong dynamics of the lepton constituents is unknown, therefore, we employ a model-independent analysis of the effects of fermion compositeness based on effective Lagrangian techniques. In this work, we assume that the excited fermions have spin and isospin $\frac{1}{2}$ since the last assignment allows the excited fermions to acquire their masses prior to $SU(2) \otimes U(1)$ breaking, avoiding dangerous bounds coming from the precise determinations of $\Delta\rho$. In the case of the first generation leptons, the assumed lightest particle spectrum is

$$l_L = \begin{bmatrix} \nu_e \\ e \end{bmatrix}_L \quad ; \quad e_R \quad : \quad L_L = \begin{bmatrix} \nu_e^* \\ e^* \end{bmatrix}_L \quad ; \quad L_R = \begin{bmatrix} \nu_e^* \\ e^* \end{bmatrix}_R \quad . \quad (3)$$

The Lagrangian describing the transition between ordinary and excited fermions should exhibit chiral symmetry in order to protect the light leptons from acquiring radiatively a large anomalous magnetic moment [6]. The $SU(2) \otimes U(1)$ invariant Lagrangian describing the interaction between excited and ordinary leptons is [7]

$$\mathcal{L}_{ll^*} = \frac{1}{2\Lambda} \bar{L}_R \sigma^{\mu\nu} \left[g f \frac{\vec{\tau}}{2} \vec{W}_{\mu\nu} + g' f' \frac{Y}{2} B_{\mu\nu} \right] l_L + h.c. \quad , \quad (4)$$

where Λ is the compositeness scale while g and g' are, respectively, the $SU(2)_L$ and $U(1)_Y$ coupling constants. Here the constants f and f' are weight factors which can be interpreted as different scales $\Lambda_i = \Lambda/f_i$ for the gauge groups. As usual, the tensors $\vec{W}_{\mu\nu}$ and $B_{\mu\nu}$ represent the field-strength tensors. Notice that our hypothesis implies that only the right-handed part of the excited fermions takes part in the generalized magnetic interaction with the known leptons.

In the physical basis, the Lagrangian (4) can be written as

$$\mathcal{L}_{ll^*} = \frac{e_0}{2\Lambda} (f - f') N_{\mu\nu} \sum_{l=\nu_e, e} \bar{l}^* \sigma^{\mu\nu} l_L + \frac{e_0}{2\Lambda} f \sum_{l, l'=\nu_e, e} \Theta_{\mu\nu}^{\bar{l}^*, l} \bar{l}^* \sigma^{\mu\nu} l' l_L + h.c. \quad , \quad (5)$$

where l (l^*) stands for ν_e or e (ν_e^* or e^*) and e_0 is the proton electric charge. The first term contains only triple vertices with $N_{\mu\nu} = \partial_\mu A_\nu - (s_w/c_w) \partial_\mu Z_\nu$ and it vanishes for $f = f'$. On the other hand, the second term contains triple as well as quartic vertices with

$$\begin{aligned}
\Theta_{\mu\nu}^{\bar{\nu}_e, \nu_e} &= \frac{1}{s_w c_w} \partial_\mu Z_\nu - i \frac{e}{s_w^2} W_\mu^+ W_\nu^- , \\
\Theta_{\mu\nu}^{\bar{e}, e} &= - \left(2\partial_\mu A_\nu + \frac{c_w^2 - s_w^2}{s_w c_w} \partial_\mu Z_\nu - i \frac{e}{s_w^2} W_\mu^+ W_\nu^- \right) , \\
\Theta_{\mu\nu}^{\bar{\nu}_e, e} &= \frac{\sqrt{2}}{s_w} \left[\partial_\mu W_\nu^+ - i e W_\mu^+ \left(A_\nu + \frac{c_w}{s_w} Z_\nu \right) \right] , \\
\Theta_{\mu\nu}^{\bar{e}, \nu_e} &= \frac{\sqrt{2}}{s_w} \left[\partial_\mu W_\nu^- + i e W_\mu^- \left(A_\nu + \frac{c_w}{s_w} Z_\nu \right) \right] .
\end{aligned} \tag{6}$$

Adding all the contributions, the chiral Vl^*l vertex is

$$\Gamma_\mu^{V\bar{f}^*f} = \frac{e_0}{2\Lambda} q^\nu \sigma_{\mu\nu} (1 - \gamma_5) f_V , \tag{7}$$

with $V = W, Z$, or γ and q being the incoming V momentum. The weak and electric charges, f_W, f_Z , and f_γ are

$$\begin{aligned}
f_W &= \frac{1}{\sqrt{2}s_w} f , \\
f_Z &= \frac{4I_{3L}(c_w^2 f + s_w^2 f') - 4e_f s_w^2 f'}{4s_w c_w} , \\
f_\gamma &= e_f f' + I_{3L}(f - f') ,
\end{aligned} \tag{8}$$

where e_f is the excited fermion charge in units of the proton charge, I_{3L} is its weak isospin, and s_w (c_w) is the sine (cosine) of the weak mixing angle.

We present our results using the two complementary coupling assignments $f = f'$ and $f = -f'$. For example, for the case $f = f'$ ($f = -f'$), the coupling of the photon to excited neutrinos (electrons) vanishes. In order to illustrate the changes in the phenomenology when we vary f and f' we display in Table I the branching ratios for excited electrons and neutrinos for the above choices of couplings.

III. SIGNALS AT LARGE HADRON COLLIDERS

In this paper we analyze the potentiality of the LHC to directly search for excited electrons and neutrinos via the reactions (1) and (2). The signal and backgrounds were simulated at the parton level with full tree level matrix elements, taking into account interference effects between the SM and excited lepton contributions. This was accomplished by numerically evaluating helicity amplitudes for all subprocesses using MADGRAPH [8] in the framework of HELAS [9], with the new interactions being implemented as additional Fortran routines. In our calculations we used the Martin–Roberts–Stirling Set G [MRS (G)] [10] proton structure functions with the factorization scale $Q^2 = \hat{s}$.

Let us, initially, concentrate on the case in which the produced vector boson is a γ , that is, the reactions $pp \rightarrow e^+e^-\gamma$ and $pp \rightarrow e^\pm\nu\gamma$. At tree level, these final states can be obtained through the single production of excited leptons via the Drell–Yan mechanism, followed by their radiative decays, *i.e.*

$$q\bar{q} \rightarrow Z^*/\gamma^* \rightarrow e^\pm e^{*\mp} \rightarrow e^\pm e^\mp \gamma , \quad (9)$$

$$qq' \rightarrow W^{*\pm} \rightarrow \nu e^{*\pm} + e^\pm \nu^* \rightarrow \nu e^\pm \gamma . \quad (10)$$

We applied to the above processes the following acceptance cuts

$$\begin{aligned} p_T &> 20 \text{ GeV} , \\ |\eta_{e^\pm, \gamma}| &< 2.5 , \\ \Delta R_{(e^+e^-), (e^+\gamma), (e^-\gamma)} &> 0.4 , \end{aligned} \quad (11)$$

where p_T is the transverse momentum of the visible particle or the missing transverse momentum when a neutrino is produced. η stands for the pseudo-rapidity of the visible particles and $\Delta R (= \sqrt{\Delta\eta^2 + \Delta\phi^2})$ is the separation between two of them. After applying these initial cuts, the SM cross sections are

$$\begin{aligned} \sigma_{pp \rightarrow e^+e^-\gamma} &= 1.29 \text{ pb} , \\ \sigma_{pp \rightarrow e^\pm\nu\gamma} &= 2.88 \text{ pb} . \end{aligned}$$

A natural way to extract the excited electron signal, and at the same time suppress the SM backgrounds, is to impose a cut on the $e\gamma$ invariant mass. For instance, Fig. 1(a) [(b)] contains the $e\gamma$ invariant distribution in the reaction $pp \rightarrow e^+e^-\gamma [e^\pm\nu\gamma]$ for the SM and with the inclusion of an excited electron with mass $m^* = 250 \text{ GeV}$ and $f/\Lambda = f'/\Lambda = 5 \text{ TeV}^{-1}$. From these figures we can see that it is convenient to collect the data in $e\gamma$ invariant mass bins since the signal is concentrated in a small region of this invariant mass spectrum. Therefore, we introduced the cut

$$|M_{e^\pm\gamma} - \overline{M}| < 25 \text{ GeV} , \quad (12)$$

where \overline{M} is the center of a 50 GeV invariant mass bin. Certainly this cut is ideal for excited electrons of mass $m^* = \overline{M}$. However, the cut (12) is efficient only for excited electron masses up to 1250 GeV since heavier excited electrons are rather broad resonances and we also run out of statistics. Consequently, we only considered $\overline{M} \leq 1500 \text{ GeV}$. To search for heavier excited electrons ($m^* > 1500 \text{ GeV}$), we performed a new analysis replacing the cut (12) by

$$M_{e^\pm\gamma} > 1250 \text{ GeV} . \quad (13)$$

To further reduce the SM background, we also vetoed events exhibiting Z 's decaying into e^+e^- pairs through the cut

$$M_{e^+e^-} > 120 \text{ GeV} . \quad (14)$$

Excited neutrinos contribute only to the $e^\pm\nu\gamma$ production and they can be identified by the γp_T transverse mass (M_T) distribution; see Fig. 2. Analogously to the excited electron case, we looked for an excess of events in M_T bins of 50 GeV via the additional cut

$$|M_T + 15 \text{ GeV} - \overline{M}| < 25 \text{ GeV} , \quad (15)$$

where \overline{M} is a variable parameter. This cut enhances the signal of excited neutrinos whose mass is \overline{M} . Once again, the cut (15) is efficient only for excited neutrino masses up to 1250 GeV so we restricted $\overline{M} \leq 1500$ GeV. For higher masses ($m^* > 1500$ GeV), the decay width of the excited neutrino is so large that we performed a different study replacing the cut (15) by

$$M_T > 1250 \text{ GeV} . \quad (16)$$

The above cuts (12)–(16) reduce the SM background drastically. For instance, assuming an excited lepton mass of 250 GeV ($= \overline{M}$) the SM background for the processes (1) and (2) is reduced to

$$\begin{aligned} \sigma_{pp \rightarrow e^+e^-\gamma}^{Me\gamma} &= 3.55 \text{ fb} , \\ \sigma_{pp \rightarrow e^\pm\nu\gamma}^{Me\gamma} &= 51.7 \text{ fb} , \\ \sigma_{pp \rightarrow e^\pm\nu\gamma}^{MT} &= 12.3 \text{ fb} , \end{aligned}$$

where we applied cuts (11-14) to the first two results and (11), (15) and (16) to the last one. Tables II–IV contain the cross sections of the irreducible background after cuts for several excited lepton masses where we can see that the background diminishes very fast with the increase of m^* .

At this point, it is important to consider other possible sources of background to these final states since the irreducible background has been largely reduced. For example, additional backgrounds are $pp \rightarrow e^+e^-$ jet and $pp \rightarrow e^\pm\nu$ jet, where a jet is misidentified as a photon. Taking the jet faking photon probability at the LHC to be $f_{\text{fake}} = 1/5000$ [11], we present also in Tables II–IV the expected cross section for these processes. Another possible reducible background for the process $pp \rightarrow e^\pm\nu\gamma$ is the reaction $pp \rightarrow e^+e^-\gamma$ with one of the charged leptons escaping undetected, that leads to missing transverse momentum. We also evaluated this processes, however, its cross section turns out to be negligible.

In order to quantify the LHC potential to search for excited leptons, we defined the statistical significance S of the signal

$$S = \frac{|\sigma_{\text{total}} - \sigma_{\text{back}}|}{\sqrt{\sigma_{\text{back}}}} \sqrt{\mathcal{L}} , \quad (17)$$

where \mathcal{L} is the LHC integrated luminosity, that we assumed to be 100 fb^{-1} . S can be easily evaluated using Tables II–IV and the expected signal cross section. In order to derived the attainable limits at the LHC, we assumed that the observed number of events is the one predicted by the SM.

Let us start our analysis by the search for excited electrons. In this case, we assumed that $f = f'$ in order to reduce the number of free parameters, and we imposed the cuts (11) – (14) with $\overline{M} = m^*$ to maximize the sensitivity for excited fermions of mass m^* . We display in Figure 3(a) the 95% C.L. bounds on the coupling $|f/\Lambda|$, coming from the process $pp \rightarrow e^+e^-\gamma$ ($e^\pm\nu\gamma$), as a function of the excited electron mass. As we can see, the $e^+e^-\gamma$ production leads to slightly better limits on excited electrons except at small m^* . The

combined results of these two processes are also presented in this figure and these bounds turn out to be at least an order of magnitude more stringent than the present best limits coming from the HERA experiments. Moreover, the LHC will be able to extend considerably the range of excited electron masses that can be probed (up to 2 TeV).

In the study of the excited neutrino production, we assumed $f = -f'$ that leads to a non-vanishing $\nu_e \nu_e^* \gamma$ coupling. The 95% C.L. limits on $|f/\Lambda|$ that can be obtained from the reaction $pp \rightarrow e^\pm \nu \gamma$, where we imposed the cuts (11) and (15) – (16), are shown in Figure 3(b). Notice that the limits on excited neutrinos from this process are looser (stronger) than the ones derived for excited electrons for $m^* < 1400$ (> 1400) GeV. Furthermore, these bounds are orders of magnitude more stringent than the presently available ones and they span a much larger range of excited neutrino masses.

It is also interesting to obtain a bound on the excited electron mass assuming that $f = f'$ and $f/\Lambda = 1/m^*$. In this scenario, the LHC will be able to rule out excited electrons with masses smaller than 1 TeV, at 95% C.L., through the study of either the $e^+e^-\gamma$ or $e^\pm \nu \gamma$ productions, while their combined results increase this limit by 40 GeV. This limit improves the present HERA bound (233 GeV) [4] by a factor of roughly 5. In the case of excited neutrinos, assuming $f = -f'$ and $f/\Lambda = 1/m^*$, the analysis of the $e^\pm \nu \gamma$ final state leads to $m^* > 838$ GeV at 95% C.L.. Again, this limit is much more restrictive than the available HERA one (~ 150 GeV).

Note that for the choice $f = f'$ ($f = -f'$), the coupling of excited neutrinos (electrons) to photons vanishes. In this way, the production of a pair of leptons ee or $e\nu$ with a photon can probe only the excited electron (neutrino) production if $f = f'$ ($f = -f'$). Therefore, we should also consider the excited lepton decay into a W or a Z and an ordinary lepton in these cases. Taking into account only the leptonic decay of the weak gauge bosons, we also analyzed the processes $pp \rightarrow e^+e^-e^+e^-$ and $e^+e^-e^\pm \nu$. Notice that excited electrons can contribute to both reactions, while excited neutrinos only to the second one.

In order to look for excited electrons in the $e^+e^-e^+e^-$ and $e^+e^-e^\pm \nu$ productions, we applied initially the acceptance cut (11) and then required

$$M_{e^+e^-} > 20 \text{ GeV} \quad (18)$$

for all possible e^+e^- pairs. This cut reduces the SM contribution due to photon exchange. The SM background to the $e^+e^-e^+e^-$ production receives a large contribution from the Z pair production and it can be further suppressed by vetoing events that exhibit two e^+e^- pairs compatible with being a Z , *i.e.*

$$\begin{aligned} |M_{e_1^+e_1^-} - m_Z| < 25 \text{ GeV} \text{ and } |M_{e_2^+e_2^-} - m_Z| < 25 \text{ GeV} \\ \text{or} \\ |M_{e_1^+e_2^-} - m_Z| < 25 \text{ GeV} \text{ and } |M_{e_1^+e_2^+} - m_Z| < 25 \text{ GeV}, \end{aligned} \quad (19)$$

where e_1^\pm (e_2^\pm) is the electron/positron with the highest (smallest) energy.

The SM background for the excited neutrino search in the $e^+e^-e^\pm \nu$ channel can be depleted by requiring that the transverse mass calculated using all charged leptons satisfy

$$M_{T_{e\nu}} > 20 \text{ GeV}. \quad (20)$$

Another important SM contribution to this reaction is WZ production with the Z decaying into a pair e^+e^- and the W decaying into a pair $e\nu$. In order to reject this process, we vetoed events displaying a pair e^+e^- compatible with being a Z and the invariant mass of the remaining e^\pm close to the W mass, *i.e.*

$$|M_{e^\pm e^\mp} - m_Z| < 25 \text{ GeV} \text{ and } |M_{T_{e^\pm \nu}} - m_W + 15 \text{ GeV}| < 25 \text{ GeV}. \quad (21)$$

Moreover, the excited electron signal in this topology originates from its charged current production in association with a neutrino. Therefore, the three charged leptons in the final state come from the decays of the excited electron. To further enhance the signal we performed the analysis considering bins in the invariant mass of the three charged leptons in the final state M_{eee} , *i.e.* we demanded that

$$|M_{eee} - \overline{M}| < 25 \text{ GeV}, \quad (22)$$

where the center of the bin \overline{M} is again a variable parameter.

We present in Figure 4(a) the attainable 95% C.L. limits on excited electrons coming from the $e^+e^-e^+e^-$ and $e^+e^-e^\pm\nu$ reactions, assuming that $f/\Lambda = f'/\Lambda$ and $f/\Lambda = -f'/\Lambda$. As we can see, the bounds for $f/\Lambda = f'/\Lambda$ are an order of magnitude weaker than the ones originating from the decay of the excited electron into a photon–electron pair. Notwithstanding, these processes are important when this decay channel is closed. As expected, the four lepton bounds for $f/\Lambda = -f'/\Lambda$ are $\mathcal{O}(20)\%$ more restrictive than the ones for $f/\Lambda = f'/\Lambda$.

The charged current production of excited neutrinos can contribute only to the $e^+e^-e^\pm\nu$ final state. The decay of the excited neutrino either in eW or in νZ leads to $e^+e^-\nu$ once we consider the W and Z decay into first family leptons. Therefore, the transverse mass of the e^+e^-

$$M_{T_{ee\nu}} = \sqrt{2(p_{T_{ee}}p_{T_{miss}} - \vec{p}_{T_{ee}} \cdot \vec{p}_{T_{miss}})} \quad , \quad (23)$$

where $p_{ee} = p_{e^+} + p_{e^-}$ and $p_{T_{ee}}$ is its transverse momentum, characterizes the excited neutrino production. In order to isolate the excited neutrino signal in the $e^+e^-e^\pm\nu$ topology, we initially applied the cuts (11), (18), and (20) and then we required the event to present an e^+e^- pair with a transverse mass in the bin

$$|M_{T_{ee\nu}} + 15 \text{ GeV} - \overline{M}| < 25 \text{ GeV}, \quad (24)$$

with \overline{M} being a variable parameter that enhances the search for excited neutrinos with mass $m^* = \overline{M}$.

We present in Figure 4(b) the attainable 95% C.L. limits on excited neutrinos coming from the $e^+e^-e^\pm\nu$ reaction, assuming that $f/\Lambda = f'/\Lambda$ and $f/\Lambda = -f'/\Lambda$. As we can see, these bounds are an order of magnitude weaker than the ones coming from the decay of the excited neutrino into a photon–neutrino pair for $f = -f'$.

IV. SUMMARY AND CONCLUSIONS

We analyzed the potential of the LHC to unravel the existence of excited leptons through the study of the processes (1) and (2). We assumed a center-of-mass energy of 14 TeV and an integrated luminosity of 100 fb^{-1} in our calculations. The final states containing a photon ($e^+e^-\gamma$ or $e^\pm\nu\gamma$) lead to the most stringent bounds, as can be seen in Figure (3), provided the excited lepton (ℓ^*) has a sizable branching ratio into pairs $\ell\gamma$. Otherwise, the search for excited leptons should be carried out studying the final states $e^+e^-e^+e^-$ and $e^+e^-e^\pm\nu$ where our results are presented in Figure (4). We also considered the possibility of the V boson in the processes (1) and (2) decaying into muons, however the improvement in the bounds is marginal.

For light excited leptons ($m^* \lesssim 200 \text{ GeV}$), the attainable limits at the LHC are less stringent than the bounds originating from LEP [5], but they are comparable to the limits obtained by HERA [4]. Notwithstanding, the LHC bounds are much stronger than the presently available ones for a large range of excited lepton masses (up to 2 TeV), being at least one order of magnitude better. Furthermore, assuming $f = f'$ and $f/\Lambda = 1/m^*$, the LHC will be able to exclude the existence of excited leptons with masses up to 1 TeV. A similar sensibility can be reached at the Next Linear Collider (NLC) [12].

In our analysis, we assumed that the excited leptons interact with the SM particles via the effective operator (4). This is a conservative assumption since it is possible that excited fermions may also couple to ordinary quarks and leptons via contact interactions originating from the strong constituent dynamics. In this case, the production cross section should be enhanced [13]. However, the contact interactions also modify the Drell-Yan process and can be strongly constrained if no deviation from the SM predictions is observed in this process.

ACKNOWLEDGMENTS

This work was supported by Conselho Nacional de Desenvolvimento Científico e Tecnológico (CNPq), by Fundação de Amparo à Pesquisa do Estado de São Paulo (FAPESP), and by Programa de Apoio a Núcleos de Excelência (PRONEX).

REFERENCES

- [1] D. Charlton, “Standard Model”, *Talk given at the International Europhysics Conference on High Energy Physics- HEP2001* (<http://www.hep2001.elte.hu/>).
- [2] For reviews and references see:
R. S. Chivukula, “Lectures on technicolor and compositeness,” arXiv:hep-ph/0011264;
W. Buchmuller, *Lectures given at 24th Int. Universitatswochen fur Kernphysik, Schladming, Austria, Feb 20 - Mar 1, 1985*;
M. E. Peskin, *Presented to 1985 Int. Symp. on Lepton and Photon Interactions at High Energies, Kyoto, Japan, Aug 19-24, 1985*;
M. Suzuki, “Survey of composite particle models of electroweak interaction,” *Based on talk given at Int. Symp. on Bound Systems and Extended Objects, Karuizawa, Japan, Mar 19-21, 1992*.
- [3] F. E. Low, *Phys. Rev. Lett.* **14**, 238 (1965);
F. Boudjema, *Int. J. Mod. Phys. A* **6**, 1 (1991);
M. E. Peskin, *Contributed to Proc. of 10th Int. Symp. on Lepton and Photon Interactions at High Energy, Bonn, West Germany, Aug 24-29, 1981*.
- [4] C. Adloff *et al.* [H1 Collaboration], *Eur. Phys. J. C* **17**, 567 (2000);
C. Adloff *et al.* [H1 Collaboration], arXiv:hep-ex/0110037;
S. Chekanov *et al.* [ZEUS Collaboration], arXiv:hep-ex/0109018.
- [5] R. Barate *et al.* [ALEPH Collaboration], *Eur. Phys. J. C* **4**, 571 (1998);
P. Abreu *et al.* [DELPHI Collaboration], *Eur. Phys. J. C* **8**, 41 (1999);
M. Acciarri *et al.* [L3 Collaboration], *Phys. Lett. B* **502**, 37 (2001);
G. Abbiendi *et al.* [OPAL Collaboration], *Eur. Phys. J. C* **14**, 73 (2000).
- [6] S. J. Brodsky and S. D. Drell, *Phys. Rev. D* **22**, 2236 (1980); F. M. Renard, *Phys. Lett. B* **116**, 264 (1982).
- [7] N. Cabibbo, L. Maiani, and Y. Srivastava, *Phys. Lett. B* **139**, 459 (1984);
J. Kuhn and P. Zerwas, *Phys. Lett. B* **147**, 189 (1984);
K. Hagiwara, D. Zeppenfeld, and S. Komamiya, *Z. Phys. C* **29**, 115 (1985);
F. Boudjema and A. Djouadi, *Phys. Lett. B* **240**, 485 (1990);
F. Boudjema, A. Djouadi, and J. L. Kneur, *Z. Phys. C* **57**, 425 (1993).
- [8] T. Stelzer and W. F. Long, *Comput. Phys. Commun.* **81**, 357 (1994).
- [9] H. Murayama, I. Watanabe, and K. Hagiwara, “HELAS: HELicity Amplitude Subroutines for Feynman diagram evaluations,” KEK-91-11.
- [10] A. D. Martin, W. J. Stirling, and R. G. Roberts, *Phys. Lett.* **B354**, 155 (1995).
- [11] H. Baer, P. G. Mercadante, F. Paige, X. Tata, and Y. Wang, *Phys. Lett. B* **435**, 109 (1998).
- [12] E. M. Gregores, M. C. Gonzalez-Garcia, and S. F. Novaes, *Phys. Rev. D* **56**, 2920 (1997).
- [13] U. Baur, M. Spira, and P. M. Zerwas, *Phys. Rev. D* **42**, 815 (1990);
O. Çakir, C. Leroy and R. Mehdiyev, ATL-PHYS-2001-015.

TABLES

$m^*(\text{GeV})$	$e^* \rightarrow e\gamma$	$e^* \rightarrow eZ$	$e^* \rightarrow \nu W$	$\nu^* \rightarrow \nu\gamma$	$\nu^* \rightarrow \nu Z$	$\nu^* \rightarrow eW$
100	0.728 (0.)	0.012 (0.137)	0.260 (0.863)	0. (0.728)	0.137 (0.012)	0.863 (0.260)
250	0.317 (0.)	0.103 (0.381)	0.580 (0.619)	0. (0.317)	0.381 (0.103)	0.619 (0.580)
500	0.289 (0.)	0.111 (0.391)	0.600 (0.609)	0. (0.289)	0.391 (0.111)	0.609 (0.600)
750	0.284 (0.)	0.113 (0.393)	0.603 (0.607)	0. (0.284)	0.393 (0.113)	0.607 (0.603)
1000	0.282 (0.)	0.113 (0.393)	0.605 (0.607)	0. (0.282)	0.393 (0.113)	0.607 (0.605)

TABLE I. Branching ratios of excited leptons with the coupling constant assignment $f = f' \neq 0$ ($f = -f' \neq 0$). Notice that the branching ratios do not depend on the value of Λ .

\overline{M} (GeV)	$pp \rightarrow e^+e^-\gamma$	$pp \rightarrow e^+e^- \text{jet}$	total
100	31.43	0.18	31.61
250	3.55	0.04	3.59
500	0.279	0.004	0.283
750	0.051	0.001	0.052
1000	0.0139	0.0002	0.0141
1250	0.0048	0.0001	0.0049
1500 - 2500	0.0243	0.0004	0.0247

TABLE II. Cross sections in fb of the irreducible and jet faking photon backgrounds for the process $pp \rightarrow e^+e^-\gamma$ after cuts (11) and (14). For \overline{M} up to 1500 GeV, the invariant mass cut (12) was also imposed while for higher \overline{M} the invariant mass cut (13) was applied.

\overline{M} (GeV)	$pp \rightarrow e^\pm\nu_{e^\pm}\gamma$	$pp \rightarrow e^\pm\nu_{e^\pm} \text{jet}$	total
100	768.0	53.9	821.9
250	51.65	2.94	54.59
500	3.54	0.17	3.71
750	0.74	0.03	0.77
1000	0.23	0.01	0.24
1250	0.087	0.002	0.089
1500 - 2500	0.54	0.01	0.55

TABLE III. Cross sections in fb of the irreducible and jet faking photon backgrounds for the process $pp \rightarrow e^\pm\nu_{e^\pm}\gamma$ after the cuts (11). For \overline{M} up to 1500 GeV, the invariant mass cut (12) was also applied while for higher \overline{M} the invariant mass cut (13) was imposed.

\overline{M} (GeV)	$pp \rightarrow e^\pm \nu_{e^\pm} \gamma$	$pp \rightarrow e^\pm \nu_{e^\pm} \text{ jet}$	total
100	857.3	68.3	925.6
250	12.25	2.20	14.45
500	0.57	0.13	0.70
750	0.08	0.02	0.10
1000	0.017	0.005	0.022
1250	0.004	0.001	0.005
1500 - 2500	0.029	0.007	0.036

TABLE IV. Cross sections in fb of the irreducible and jet faking photon backgrounds for the process $pp \rightarrow e^\pm \nu_{e^\pm} \gamma$ after the cuts (11). For \overline{M} up to 1500 GeV, the invariant mass cut (15) was also used, while for higher \overline{M} the invariant mass cut (16) was applied.

FIGURES

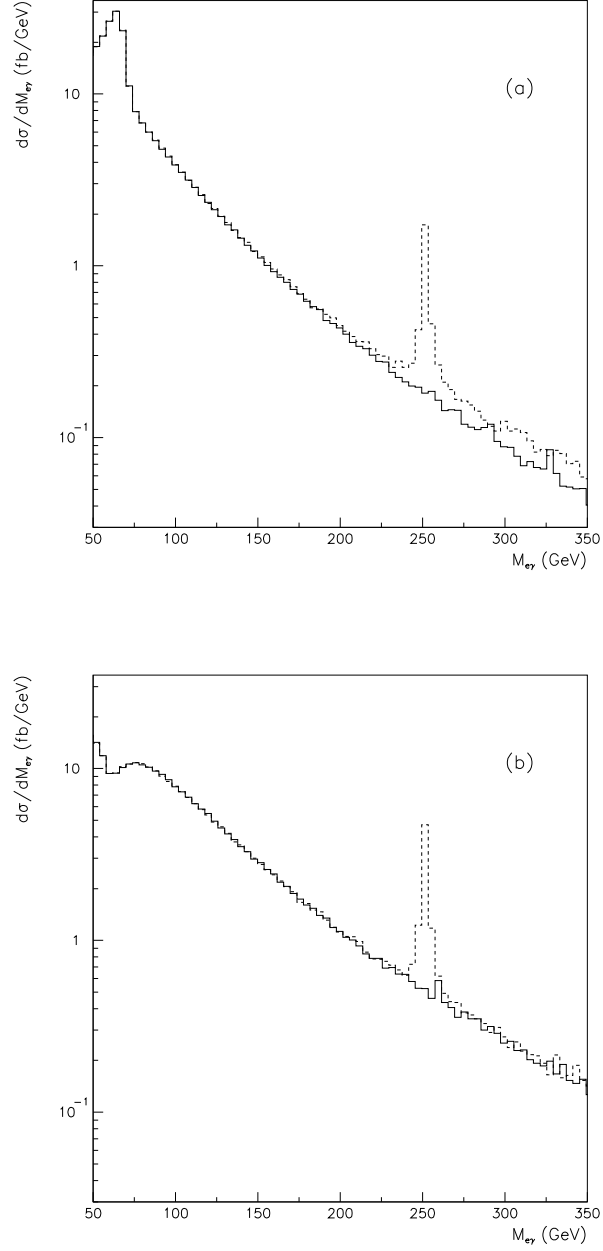


FIG. 1. Invariant mass distribution of the pair $e\gamma$ in the process $pp \rightarrow e^+e^-\gamma$ (a) and $pp \rightarrow e^\pm\nu\gamma$ (b). The full line stands the SM background and the dashed line for the excited electron signal, assuming $m^* = 250$ GeV and $f/\Lambda = f'/\Lambda = 5/\text{TeV}$.

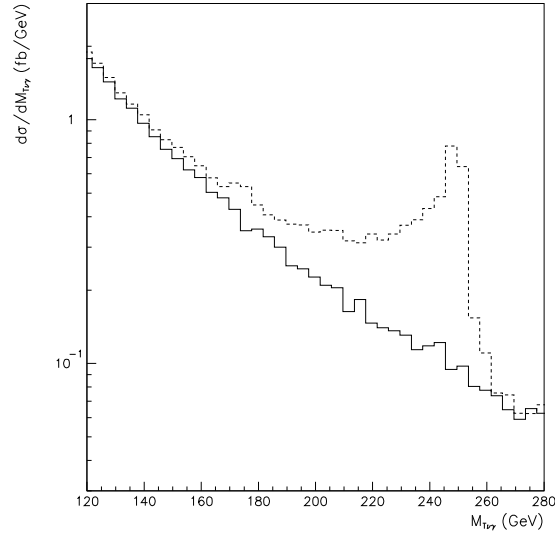


FIG. 2. Transverse mass distribution in the reaction $pp \rightarrow e\nu\gamma$ at LHC. The full line represents the SM background while the dashed line stands for an excited neutrino signal, assuming $m^* = 250$ GeV and $f/\Lambda = f'/\Lambda = 5/\text{TeV}$.

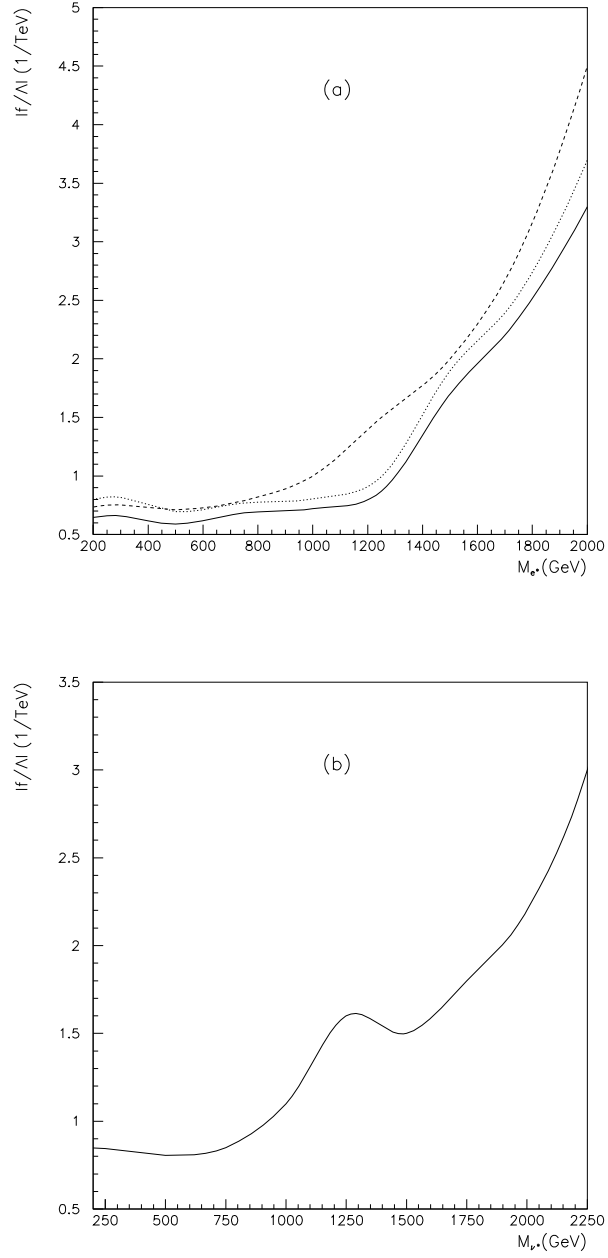


FIG. 3. 95% C.L. limits on the coupling $|f/\Lambda|$ of excited electrons (a) and excited neutrinos (b). In (a) the dotted (dashed) line stands for the bounds coming from the $pp \rightarrow e^\pm \nu \gamma$ ($e^+ e^- \gamma$) reaction while the solid line represents the combined results. In (b), the solid line displays the bounds coming from the process $pp \rightarrow e^\pm \nu \gamma$.

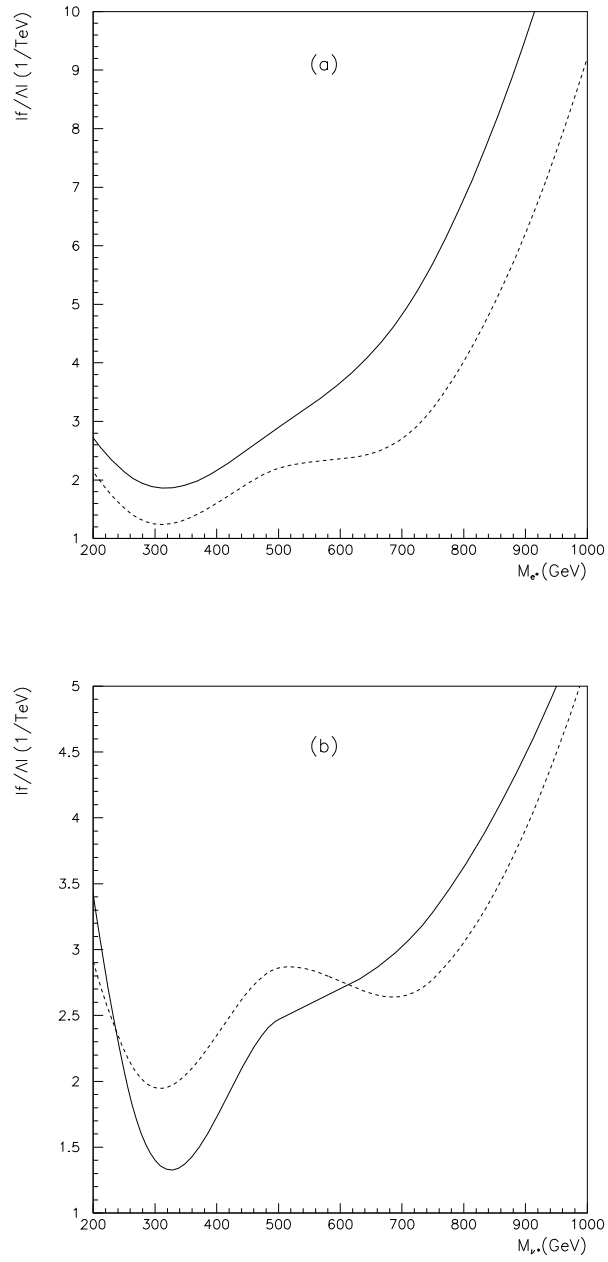


FIG. 4. 95% C.L. limits on the coupling $|f/\Lambda|$ of excited electrons (a) and excited neutrinos (b) obtained by combining the searches in the reactions $pp \rightarrow e^+e^-e^\pm\nu$ and $pp \rightarrow e^+e^-e^+e^-$. The solid (dashed) line stands for the coupling assignment $f = f'$ ($f = -f'$).